ChemPubSoc Europe

DOI: 10.1002/chem.201505162

CHEMISTRY A European Journal Full Paper

Lewis Acid Catalysis

Addition Reactions of Me_3SiCN with Aldehydes Catalyzed by Aluminum Complexes Containing in their Coordination Sphere O, S, and N Ligands

Zhi Yang,*[a, b] Yafei Yi[+],[a] Mingdong Zhong[+],[a] Sriman De,[c] Totan Mondal,[c] Debasis Koley,*[c] Xiaoli Ma,[a] Dongxiang Zhang,[a] and Herbert W. Roesky*[d]

Abstract: The reaction of one equivalent of $LAlH_2$ (**1**; L = $HC(CMeNAr)_2$, Ar = 2,6-*i*$Pr_2C_6H_3$, β-diketiminate ligand) with two equivalents of 2-mercapto-4,6-dimethylpyrimidine hydrate resulted in $LAl[(\mu\text{-}S)(m\text{-}C_4N_2H)(CH_2)_2]_2$ (**2**) in good yield. Similarly, when *N*-2-pyridylsalicylideneamine, *N*-(2,6-diisopropylphenyl)salicylaldimine, and ethyl 3-amino-4,5,6,7-tetrahydrobenzo[*b*]thiophene-2-carboxylate were used as starting materials, the corresponding products $LAl[(\mu\text{-}O)(o\text{-}C_6H_4)\text{-}CN(C_5NH_4)]_2$ (**3**), $LAlH[(\mu\text{-}O)(o\text{-}C_4H_4)CN(2,6\text{-}iPr_2C_6H_3)]$ (**4**), and $LAl[(\mu\text{-}NH)(o\text{-}C_8SH_8)(COOC_2H_5)]_2$ (**5**) were isolated. Compounds **2**–**5** were characterized by ^1H and ^{13}C NMR spectroscopy as well as by single-crystal X-ray structural analysis. Surprisingly, compounds **2**–**5** exhibit good catalytic activity in addition reactions of aldehydes with trimethylsilyl cyanide (TMSCN).

Introduction

The Lewis acid properties of organic aluminum compounds are well established in organic chemistry. They are responsible for a plethora of organic reactions,[1] polymerizations,[2] and catalytic cycles.[3–6] Among those compounds, Lewis acidic derivatives prepared from $AlCl_3$ are primarily used, although poor selectivity and control of reactivity are often the major issues in using these compounds.[4,7] Increasing the selectivity of these compounds and controlling their reactivity can be achieved by increasing the steric bulk and by varying the electron density at the central aluminum atom. For thermodynamic stability reasons, aluminum compounds containing O, S, and N ligands have been less-well studied compared with aluminoxanes. Since the first unique monomeric aluminum moiety comprising the terminal Al–SH unit was reported,[8] more and more soluble organic Al–S bond containing compounds have been synthesized.[9] The use of organic aluminum compounds for the mediation of various organic transformations has a long-standing tradition,[4,5,10] and aluminum-mediated organic reactions have been extensively reviewed.[4,5,7,11] The β-diketiminate substituent has found widespread applications as a supporting ligand owing to its strong electron-donating ability and steric constraints that can stabilize main-group metal compounds.[12] However, aluminum compounds with chelating ligands incorporating soft donors that can be as moderate and stable Lewis acid catalysts are less known.[13]

Monomeric aluminum hydrides with an electron-withdrawing and bulky group, which increases the positive charge at the aluminum center, are relatively rare and few of these compounds have been structurally characterized.[14,12a] Recently, we reported an aluminum hydride, LAlH(OTf), (Tf = SO_2CF_3), which effectively acts as a bifunctional catalyst and initiates the addition reaction of trimethylsilyl cyanide (TMSCN) to aldehydes and ketones.[3b] Thus, to investigate the catalytic properties of aluminum compounds containing O, S, and N organic ligands is an important task.[15,16] Herein, we report the synthesis and structural characterization of four aluminum compounds with soft donor properties. Their catalytic activity was studied in the addition reaction of TMSCN to aldehydes.

Results and Discussion

The reaction of **1** with 2-mercapto-4,6-dimethylpyrimidine hydrate, *N*-2-pyridylsalicylideneamine, *N*-(2,6-diisopropylphenyl)-salicylaldimine, and ethyl 3-amino-4,5,6,7-tetrahydrobenzo[*b*]-thiophene-2-carboxylate, respectively, in a molar ratio of 1:2 or

[a] *Prof. Z. Yang, Y. Yi,[+] Dr. M. Zhong,[+] Dr. X. Ma, Dr. D. Zhang*
School of Chemical Engineering and Environment
Beijing Institute of Technology, 100081 Beijing (P. R. China)
E-mail: zhiyang@bit.edu.cn

[b] *Prof. Z. Yang*
State Key Laboratory of Elemento-organic Chemistry
Nankai University (P. R. China)

[c] *S. De, T. Mondal, Dr. D. Koley*
Department of Chemical Sciences
Indian Institute of Science Education and Research Kolkata
Mohanpur 741246 (India)
E-mail: koley@iiserkol.ac.in

[d] *Prof. H. W. Roesky*
Institut für Anorganische Chemie, Universität Göttingen
Tammannstrasse 4, 37077 Göttingen (Germany)
E-mail: hroesky@gwdg.de

[+] *These authors contributed equally to this work.*

Supporting information for this article is available on the WWW under http://dx.doi.org/10.1002/chem.201505162.

1:1 resulted in products $(LAl[(\mu\text{-}S)(m\text{-pyrimidine})(CH_2)_2]_2$ (**2**), $LAl[(\mu\text{-}O)(o\text{-}C_6H_4)CN(C_5NH_4)]_2$ (**3**), $LAlH[(\mu\text{-}O)(o\text{-}C_4H_4)CN(2,6\text{-}iPr_2C_6H_3)]$ (**4**), and $LAl[(\mu\text{-}NH)(o\text{-}C_8SH_8)(COOC_2H_5)]_2$ (**5**; Scheme 1). During the course of the reactions, hydrogen gas evolution was observed. Compounds **2**, **3**, and **5** were isolated after growing colorless crystals from the concentrated toluene solution, whereas **4** was crystallized from *n*-hexane. The crystals are soluble in common organic solvents such as toluene, dichloromethane, and tetrahydrofuran. They are stable for a few days even in the open air.

All complexes were characterized by ^1H and ^{13}C NMR spectroscopic investigations in $CDCl_3$ or C_6D_6 solution. Compound **2** exhibits a resonance for the γ-H proton on the pyrimidine rings at $\delta = 6.06$ ppm, which is populated approximately in a 2:1 ratio compared with that of the γ-H proton of the free ligand at $\delta = 5.39$ ppm. A broad resonance at $\delta = 1.25$ ppm, assigned to the methyl on the pyrimidine rings, shows a downfield shift relative to the methyl ($\delta = 1.10$ ppm) on the phenyl group in **2**. The ^1H NMR spectra of **2**, **3**, and **5** exhibit one characteristic septet ($\delta = 3.06$–3.37 ppm) attributed to the symmetry-related methyne, indicating symmetric molecules. The ^1H NMR spectra of **3** and **5** each exhibit one set of resonances for the aryl groups. Compound **3** shows the C*H*=N–Ar resonance at $\delta = 9.48$ ppm. Similarly, the ^1H NMR spectrum of compound **4** exhibits a C*H*=N–Ar resonance at $\delta = 8.29$ ppm. Three septet resonances ($\delta = 3.40$–3.05 ppm) were assigned to the methyne in the ^1H NMR spectrum of **4**, and two of the three peaks are partly overlapping, which indicate an asymmetric arrangement of compound **4**. The resonances ($\delta = 3.54$ and 4.27 ppm for **5**) were assigned to the -N*H* and the -OCH_2CH$_3$ groups, respectively.

Compounds **2**–**5** were characterized by single-crystal X-ray diffraction. The molecular structures are shown in Figures S1–S4 (in the Supporting Information). Selected bond lengths and angles are listed in the legends of Figures S1–S4. In the structures of **2**, **3**, and **5**, the aluminum center is four-coordinate, and surrounded by a β-diketiminate ligand and two bridging sulfur, oxygen, or nitrogen atoms, respectively. The two Al–S bond lengths in **2** are a little different (2.2844 Å and 2.3137 Å), which could be attributed to the interaction between Al(1) and N(5) (distance 2.1208 Å; Figure S1 in the Supporting Information). In compound **4**, the aluminum atom is also four-coordinate and the Al–O bond length (1.7176 Å) is shorter than that in **3** (av. 1.7229 Å), and they are both longer than those in $LAl(OH)_2$ (1.705 Å).[17] The difference in the bond lengths of **3** and **4** compared with those in $LAl(OH)_2$ could be attributed to the conjugative effect of the O atoms with the adjacent aromatic ring as well as with the repulsive force between the bulky groups on the O atoms with those of the $iPr_2C_6H_3$ groups on the ligand.

To investigate the catalytic properties of compounds **2**–**5**, addition reactions were performed by adding TMSCN to aldehydes. As shown in Table 1, the reaction of benzaldehyde (PhCHO) with TMSCN in $CDCl_3$ in the presence of **2**, **3**, **4**, or **5** as catalysts (Table 1, entries 2b, 3a, 4a, and 5a) at ambient temperature afforded the desired product PhCH(CN)OTMS in

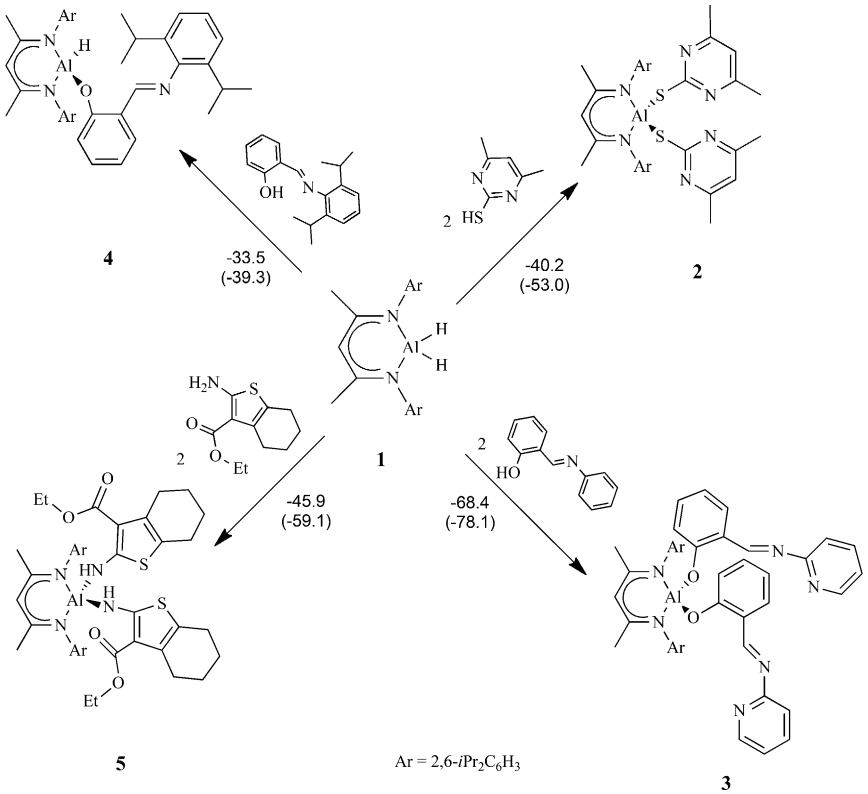

Scheme 1. Synthesis of aluminum monohydride complexes **2**, **3**, **4**, and **5** and their corresponding gas-phase free energy change (ΔG_L) and gas-phase enthalpy change (ΔH_L) values in kcal mol^{-1} calculated at the M06/def2-TZVP//BP86/def2-SVP level of theory.

Table 1. Addition reaction of TMSCN to aldehydes catalyzed by **2**, **3**, **4**, and **5**. R = alkyl or aryl group.[a]

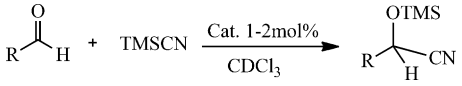

Entry	Substrate	Initiator	Cat. [mol%]	*t* [h]	Yield [%][b]
2a	C_6H_5CHO	**2**	0	4	trace
2b	C_6H_5CHO	**2**	2	4	99
2c	*p*-MeC_6H_4CHO	**2**	1.5	4	99
2d	$C_6H_5CH{=}CHCHO$	**2**	2	6	76
2e	*o*-FC_6H_4CHO	**2**	2	4	79
2f	2-C_4H_3OCHO	**2**	1	4	98
2g	2-C_4H_3SCHO	**2**	1	4	99
2h	$(CH_3)_3CHO$	**2**	2	3	99
3a	C_6H_5CHO	**3**	2	4	96
3b	*p*-MeC_6H_4CHO	**3**	1.5	4	40
3c	$C_6H_5CH{=}CHCHO$	**3**	2	6	10
3d	*o*-FC_6H_4CHO	**3**	2	4	92
3e	2-C_4H_3OCHO	**3**	1	4	30
3f	2-C_4H_3SCHO	**3**	1	4	0
3g	$(CH_3)_3CHO$	**3**	2	3	99
4a	C_6H_5CHO	**4**	2	4	95
4b	*p*-MeC_6H_4CHO	**4**	1.5	4	45
4c	$C_6H_5CH{=}CHCHO$	**4**	2	6	30
4d	*o*-FC_6H_4CHO	**4**	2	4	95
4e	2-C_4H_3OCHO	**4**	1	4	90
4f	2-C_4H_3SCHO	**4**	1	4	20
4g	$(CH_3)_3CHO$	**4**	2	3	99
5a	C_6H_5CHO	**5**	2	4	65
5b	*p*-MeC_6H_4CHO	**5**	2	4	10
5c	$C_6H_5CH{=}CHCHO$	**5**	2	6	10
5d	*o*-FC_6H_4CHO	**5**	1.5	3	99
5e	2-C_4H_3OCHO	**5**	2	4	50
5f	2-C_4H_3SCHO	**5**	2	4	15
5g	$(CH_3)_3CHO$	**5**	2	3	99

[a] Conditions: aldehyde, 1 mmol; TMSCN, 1.2 mmol; at ambient temperature. [b] Yield was obtained according to ^1H and ^{13}C NMR spectral analysis.

good yield (as determined by ^1H NMR analyses of the reaction mixture). No reaction was observed under the same conditions in the absence of the catalyst (Table 1, entry 2a). *p*-Tolylaldehyde was investigated for the addition reaction with TMSCN at room temperature by using catalyst **2** with a loading of 1.5 mol% to afford the product in essentially quantitative yield (99%, Table 1, entry 2c). Relatively lower yields of the product were observed in the presence of 2 mol% of catalyst **5**, and 1.5 mol% of catalysts **3** and **4** (Table 1, entries 3b, 4b, 5b). Phenylacrolein and *o*-fluorobenzaldehyde, with different electron-donating and electron-withdrawing abilities, were investigated to study the electronic effect on the activation using a variety of compounds. Catalyst **2** shows good catalytic activity when each of the two aldehydes were employed (Table 1, entries 2d, 2e), whereas **3**, **4**, and **5** only gave excellent yields for *o*-fluorobenzaldehyde (Table 1, entries 3d, 4d, 5d). This can be explained by the steric as well as the electronic properties of the substituents at the carbonyl functionality of the aldehydes. In addition, the interaction between the metal center and the carbonyl oxygen, sulfur, or nitrogen atoms has a strong influence on the catalytic activity. The analogous reactions with substrates including heterocycles were also found to be effective in the presence of **2** (Table 1, entries 2f, 2g). However, compounds **3**, **4**, and **5** show low catalytic activity compared with **2** (Table 1, entries 3e, 3f, 4e, 4f, 5e, 5f). Aliphatic aldehydes (Table 1, entries 2h, 3g, 4g, 5g) were selected for the addition with TMSCN at room temperature using catalyst loadings of 2 mol% and the reaction time of 3 h. The products were formed in essentially quantitative yield (99%). In general, we observed that better catalytic performance occurred with aldehydes of small molecular weight. Based on the results of Table 1, compound **2** shows high catalytic activity for all the selected aldehydes, whereas compounds **3**, **4**, and **5** exhibit high selectivity for some specific aldehydes, which might be due to the more bulky groups around the Al center of compounds **3**, **4**, and **5** than those of **2** and some other known catalysts.[3b,18] The X-ray structures of compounds **2**, **3**, **4**, and **5** are illustrated in the Supporting Information, which shows that the steric effect of the bulky groups on the Al center decreases the catalytic activity.

We next performed DFT calculations with an aim to investigate the mechanistic pathways in the addition reaction of TMSCN to PhCHO in the presence of Al^{III} catalysts (Scheme 1). Four catalysts **2**, **3**, **4**, and **5** were formed by ligand exchange from **1** by liberating H_2 gas through a highly exergonic step (Scheme 1). The respective energy changes during the formation of species **2**–**5** from initial precursor **1** are −40.2, −68.4, −33.5, and −45.9 kcal mol^{-1} (ΔG_L at the M06/def2-TZVP//BP86/def2-SVP level), indicating facile conversions. In this current contribution, only the catalytic cycle utilizing catalyst **4** is thoroughly discussed (Figure 1 and Scheme 2), however, the energies of the key intermediates for the other catalytic systems (**2**, **3**, and **5**) are collected in the Supporting Information (Figures S5–S7). As the ligands coordinated to the Al center exhibit considerable steric congestion that might hinder the progress of the substrate, we decided to dissociate one such ligand to generate a more active cationic species. Unfortunately, the ligand dissociation step from **4** is highly endoergic (ΔG_L^S = 63.8 kcal mol^{-1}, Scheme S1 in the Supporting Information), which is probably due to the electron deficiency at the Al^{III} center, proving its unlikeliness as a step in the reaction mechanism. Therefore, the reaction proceeds through initial substrate coordination to the Al center of **4**. The approach of TMSCN from the N-end to the tetrahedral Al center along the opposite side of one Al–N bond leads to the formation of an encounter adduct of the type $\mathbf{4_A}$. The weakly bound intermediate, $\mathbf{4_A}$ is less stable than the starting material comprising of **4** and TMSCN (ΔG_L^S = 4.2 kcal mol^{-1}). The calculated activation barrier for the transition state $\mathbf{4_A}$-**TS** is quite small ($\Delta^{\ddagger} G_L^S$ = 3.7 kcal mol^{-1}). The activated complex $\mathbf{4_A}$-**TS** is characterized by a single imaginary mode concerning the approach of the incoming TMSCN towards the Al atom. The Mulliken group charge of TMSCN in the transition state is 0.094 e, indicating an electron transfer from the TMSCN to the electrophilic Al center. The effect of such electron transfer is manifested with the elongation of the C^1–Si bond in $\mathbf{4_A}$-**TS** by 0.010 Å with respect to the free TMSCN. In the resulting intermediate $\mathbf{4_B}$, the Al center adopts a five-coordinate distorted trigonal-bipyramidal-like geometry (Figure 2), where the incoming N^1 (TMSCN) is

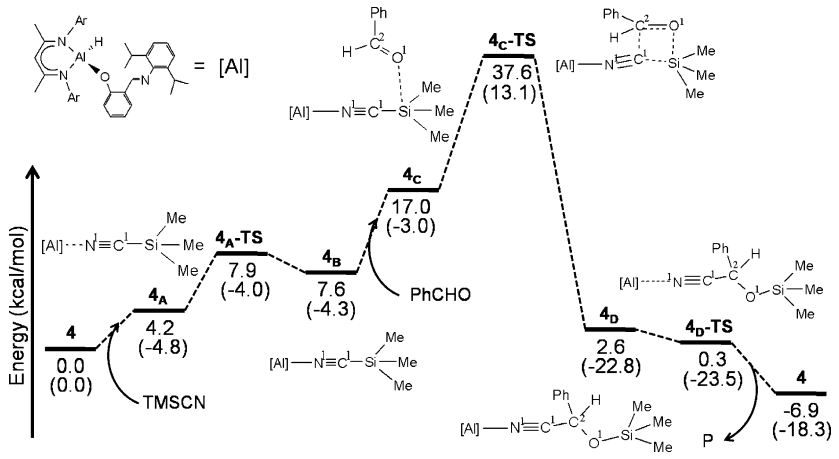

Figure 1. Energy profile for the addition reaction of TMSCN to PhCHO in the presence of catalyst **4**. The energy terms, $\Delta G_L^S/(\Delta H_L^S)$ are in kcal mol^{-1} and were calculated at the M06/def2-TZVP/SMD//BP86/def2-SVP level of theory.

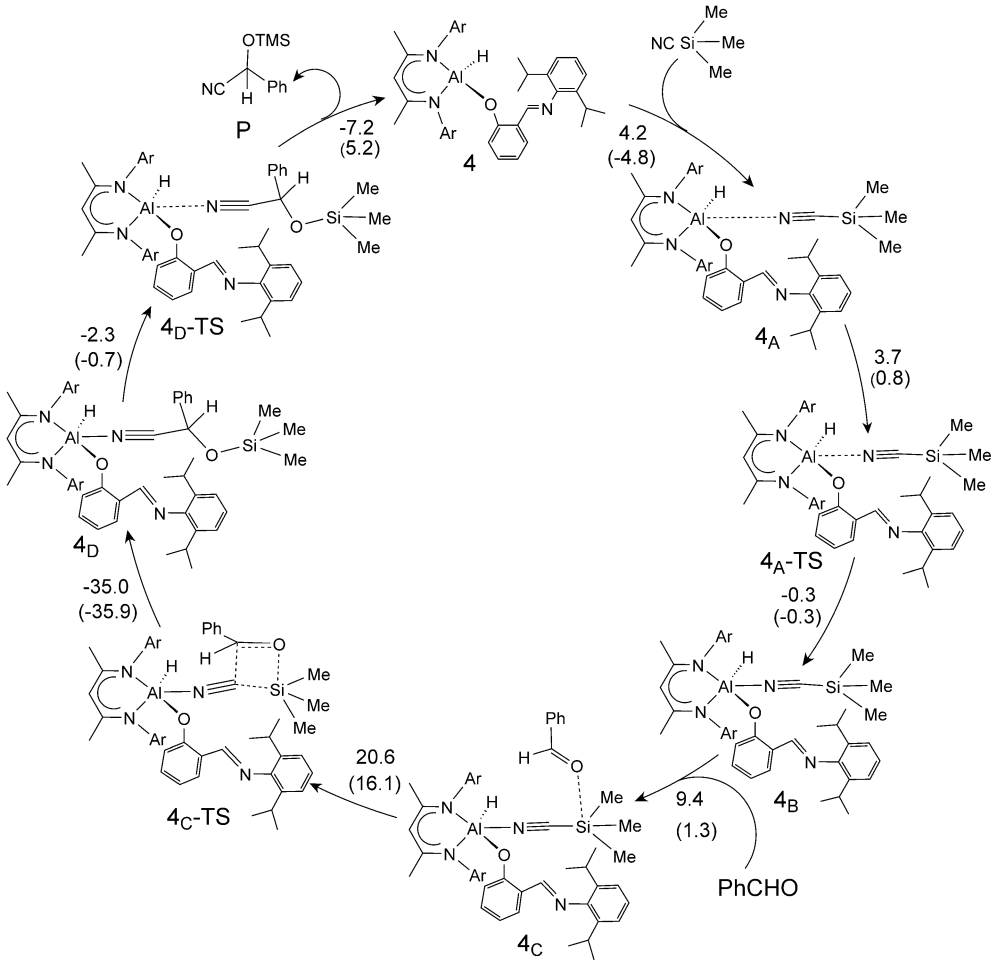

Scheme 2. Reaction mechanism for the addition reaction of TMSCN to PhCHO in the presence of the catalyst **4**. For energy conventions, refer to Figure 1.

in an axial position. During this nucleophilic addition of TMSCN (**4**→**4$_B$**), the Mulliken charge of the Al center is reduced by 0.119 e (Table 2, Table S2 in the Supporting Information). An alternative route of initial nucleophilic attack by PhCHO to the Al center was not considered because of the formation of an unrealistic geometry as reported in a previous contribution.[3b]

Interestingly, the C^1–Si bond of TMSCN is elongated by 0.025 Å in **4$_B$**, because the electron density of the -C^{1}N^1 group in TMSCN is delocalized to the Al center and the charge sepa-

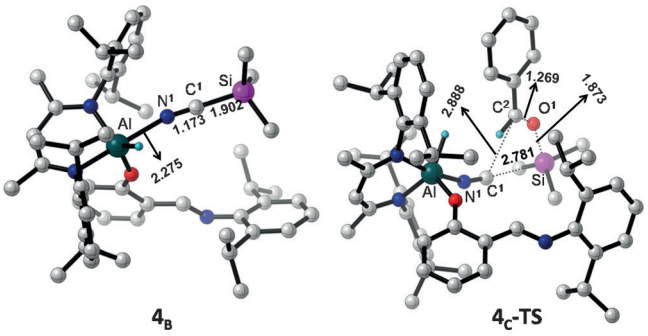

Figure 2. Optimized geometry of $\mathbf{4_B}$ and $\mathbf{4_C}$-**TS** at the BP86/def2-SVP level of theory.

Table 2. The Mulliken charges (e) of selected atoms in selected intermediates and reactants.

	Al	N^1	C^1	Si	C^2	O^1
PhCHO					0.398	−0.435
o-FC_6H_4CHO					0.400	−0.434
p-MeC_6H_4CHO					0.384	−0.441
TMSCN		−0.233	−0.088	0.440		
$\mathbf{4_B}$	−0.126	−0.144	0.053	0.400		
$\mathbf{4_C}$	−0.132	−0.169	0.102	0.363	0.388	−0.458
$\mathbf{4_D}$	−0.228	−0.110	−0.055	0.433	0.397	−0.402

ration of the Si and -C^1N^1 group is increased by 0.190 e from free TMSCN (Table 2). Therefore, the weaker C^1–Si bond is now able to undergo activation by the carbonyl compound. The addition of PhCHO to the intermediate $\mathbf{4_B}$ results in another weakly bound complex, $\mathbf{4_C}$, which may not be sustained in the condensed phase. The formation of $\mathbf{4_C}$ is endergonic (ΔG_L^S = 9.4 kcal mol^{-1}) owing to the entropic energy during the association. Species $\mathbf{4_C}$ then undergoes cycloaddition of C^1–Si with the C^2=O^1 bond of the incoming PhCHO through a four-membered cyclic transition state, $\mathbf{4_C}$-**TS** (Figure 1). The cyanohydrin is already formed and remains coordinated to the Al center in the resulting intermediate $\mathbf{4_D}$. This step corresponds to an activation barrier of 30.0 kcal mol^{-1}. The transition state vector depicts a single imaginary mode of the C^1–Si bond cleavage and concomitant formation of the C^1–C^2 and O^1–Si bonds. The increased C^1–Si and C^1–O^1 bond lengths in $\mathbf{4_C}$-**TS** amount to 2.781 and 1.269 Å, respectively (Figure 2). The overall insertion step is exergonic [$\Delta G_L^S(\mathbf{4_B}\rightarrow\mathbf{4_D})$ = −5.0 kcal mol^{-1}] and also highly exothermic [ΔH_L^S = −18.5 kcal mol^{-1}], suggesting an adequate thermodynamic driving force for $\mathbf{4_D}$ formation. Finally, there is a very shallow PES (potential energy surface) found in the product decoordination step. The calculated transition state $\mathbf{4_D}$-**TS** is lower than the intermediate $\mathbf{4_D}$ by 2.3 kcal mol^{-1}, signifying a barrierless, facile ligand dissociation step to furnish the desired product and to regenerate the catalyst **4** (Figure 1).

In the reaction pathway described in Figure 1, the highest activation barrier ($\Delta^{\ddagger}G_L^S$ = 30.0 kcal mol^{-1}) is required for the insertion step, which is referred to as the rate-determining step. Therefore, the rate-determining step is governed by nucleophilic charge transfer from C^1 to C^2 and thus the reaction rate should be faster for more electronic charge on C^1 in the X_B intermediate (X = 2 to 5) and less on C^2 of the aldehyde and vice versa. The C^2 center of *p*-MeC_6H_4CHO is relatively more electron rich than that of PhCHO and *o*-FC_6H_4CHO (Table 2), resulting in the slower reaction rate compared with the other two. For catalysts **3**, **4**, and **5**, the reaction of *p*-MeC_6H_4CHO results in product formation with very poor yields (that is, 40, 45, and 10%, respectively). However, this observation does not hold for catalyst **2**, where excellent product yield (99%) is reported under experimental conditions. This is due to the very high electron density at the C^1 center of $\mathbf{2_B}$ [$q_{C1}(\mathbf{2_B})$ = −0.041 e], which provides sufficient driving force for the nucleophilic attack at the C^2 center of the aldehyde.

We have reported similar investigations of TMSCN addition to PhCHO in the presence of the other three catalysts **2**, **3**, and **5**. The three energy profiles including the optimized intermediates are drawn in Figures S5–S7 (in the Supporting Information). All the corresponding intermediates connecting to the catalytic pathways for catalysts **2**, **3**, and **5** are higher in energy than that of catalyst **4** owing to the greater steric influence of the bulky ligands at the Al center (Figure S8 in the Supporting Information). Generally, the relative energies of the intermediates for all the computed catalytic systems (**2**–**5**) follow the trend: **4** < **3** < **5** < **2**, except that of the intermediate $\mathbf{5_B}$, which is slightly more stabilized than $\mathbf{3_B}$.

Conclusion

Four Lewis acidic aluminum compounds **2**, **3**, **4**, and **5** have been synthesized and fully characterized by single-crystal X-ray structural analysis. Compounds **2**–**5** each contain in their coordination sphere a β-diketiminate ligand and two bridging sulfur, oxygen, or nitrogen atoms, respectively, at the aluminum center. They efficiently catalyze the addition reactions of trimethylsilyl cyanide (TMSCN) to aldehydes. DFT studies reveal that the reaction proceeds through a stepwise mechanism via an intermediate, $\mathbf{4_B}$, where the C^1–Si bond in the coordinated TMSCN is lengthened as a result of adequate charge separation between the C^1 and Si atoms. The polarized C^1–Si bond is then activated by addition to the C=O group of the aldehyde. Further exploration of the detailed mechanistic studies for all catalysts (**2**–**5**) are currently in progress in our laboratory.

Experimental Section

General information

Unless otherwise noted, all manipulations were performed by using a vacuum line and standard Schlenk techniques with an atmosphere of nitrogen or by using glovebox techniques. All solvents, including $CDCl_3$ and C_6D_6, were heated at reflux over the appropriate drying agent and distilled prior to use. ^1H and ^{13}C NMR spectra were recorded with a Varian Mercury Plus 400 MHz. Commercially available chemicals were purchased from Alfa and used as received. LH[19] and $LAlH_2$[20] were prepared as described in the literature.

Synthesis of 2

A solution of **1** (0.446 g, 1.0 mmol) in toluene (10 mL) was added drop by drop to a solution of 2-mercapto-4,6-dimethylpyrimidine hydrate (0.283 g, 2 mmol) in toluene (15 mL) at 0 °C. After the addition was complete, the reaction mixture was allowed to warm to room temperature and stirring was continued for 12 h to give a white suspension, which was filtered. The crude product was crystallized from toluene to afford colorless crystals of **2**. An additional crop of **2** was obtained from the mother liquor. Total yield: 0.621 g (86%); m.p.: 240.3–241.2 °C; ^{1}H NMR (400 MHz, $CDCl_3$, 25 °C, TMS): δ = 7.25–7.09 (m, 8H, Ar-*H*), 6.06 (br, 2H, γ-*H*), 5.39 (s, 1H, γ-*H*), 3.37 (br, 4H, C*H*Me$_2$), 1.82 (br, 12H, Pyr-*Me*), 1.25 (br, 6H, *Me*), 1.10 ppm (br, 24H, CH*Me*$_2$); ^{13}C NMR (101 MHz, $CDCl_3$, 25 °C, TMS): δ = 170.3 (Pyr-NCN), 166.1 (Pyr-*C*=N), 161.9 (*C*=N), 144.9 (*o*-Ar), 142.5 (*o*-Ar), 140.7 (*i*-Ar), 129.0, 128.2, 126.7, 126.5, 125.1, 124.0, 123.0 (*C* of Ar), 114.3 (γ-Pyr), 93.2 (γ-*C*), 28.6, 28.2 (*C*HMe$_2$), 25.4, 25.2, 24.9, 24.2, 23.2, 22.7, 20.7 ppm (*Me*); elemental analysis calcd (%) for $C_{41}H_{55}AlN_6S_2$ (M_r = 723.01): C 68.11, H 7.67, N 11.62; found: C 68.44, H 7.60, N 11.72.

Synthesis of 3

Compound **3** was prepared in a similar manner to **2** from **1** (0.446 g, 1.0 mmol) and *N*-2-pyridylsalicylideneamine (0.396 g, 2 mmol). The crude product was crystallized from toluene to afford colorless crystals of **3**, and the extract was stored at room temperature for 2 d to afford **3** as colorless crystals. An additional crop of **3** was obtained from the mother liquor. Total yield: 0.586 g (70%); ^{1}H NMR (400 MHz, $CDCl_3$, 25 °C, TMS): δ = 9.48 (s, 2H, C*H*=N), 8.40-–6.66 (m, 22H, Ar-*H*) 5.37 (s, 1H, γ-*H*), 3.06 (sept, 4H, C*H*Me$_2$), 1.94 (s, 6H, *Me*), 1.23 (d, *J* = 6.8 Hz, 12H, CH*Me*$_2$), 1.13 ppm (d, *J* = 6.8 Hz, 12H, CH*Me*$_2$); ^{13}C NMR (101 MHz, $CDCl_3$, 25 °C, TMS): δ = 164.79 (*C*H=N), 161.92, 161.20, 157.61 (*C*=N), 148.99, 142.46, 140.73, 138.49, 133.86, 133.50, 129.05, 128.24, 125.08, 123.02, 120.49, 119.23, 117.29 (*C* of Ar and Pyr), 93.24 (γ-*C*), 28.19 (*C*HMe$_2$), 24.24, 23.22 (CH*Me*$_2$), 20.75 ppm (β-*Me*); elemental analysis calcd (%) for $C_{53}H_{59}AlN_6O_2$ (M_r = 839.06): C 75.87, H 7.09, N 10.02; found: C 76.33, H 7.21, N 9.78.

Synthesis of 4

Compound **4** was prepared in a similar manner to **2** from **1** (0.446 g, 1.0 mmol) and *N*-(2,6-diisopropylphenyl)salicylaldimine (0.282 g, 1.0 mmol). The crude product was crystallized from *n*-hexane to afford colorless crystals of **4**. The solvent was removed in vacuo. The solid was extracted with *n*-hexane (15 mL), and the extract was stored at room temperature for 1 d to afford **4** as colorless crystals. An additional crop of **4** was obtained from the mother liquor. Total yield: 0.429 g (58%); m.p.: 212–215 °C; IR (KBr): ν = 1740 cm^{-1}(d, Al-H); ^{1}H NMR (400 MHz, C_6D_6, 25 °C): δ = 8.29 (s, 1H, C*H*=N), 7.17-–6.81 (m, 13H, Ar-*H*), 4.97 (s, 1H, γ-*H*), 3.35 (sept, 2H, C*H*Me$_2$), 3.19–3.07 (m, 4H, C*H*Me$_2$), 2.01 (s, 3H, *Me*), 1.65 (s, 3H, *Me*), 1.33–1.31 (m, 18H, CH*Me*$_2$), 1.28–1.21 (m, 12H, CH*Me*$_2$), 1.11–1.09 (m, 3H, CH*Me*$_2$), 1.03–1.01 ppm (m, 3H, CH*Me*$_2$); ^{13}C NMR (101 MHz, C_6D_6, 25 °C): δ = 171.02 (CH=N), 159.61 (C=N), 159.41 (C=N), 144.15, 142.13, 140.89, 138.92, 137.31, 131.75, 128.82, 127.58, 127.01, 126.57, 125.52, 125.31, 124.28, 124.21, 124.02, 123.44, 123.35, 122.68 (*C* of Ar), 97.06 (γ-*C*), 28.20, 27.91, 27.90 (*C*HMe$_2$), 24.70, 24.35, 24.14, 23.97, 23.12, 23.06, 22.90 ppm (*C*H$_3$); elemental analysis calcd (%) for $C_{48}H_{64}AlN_3O$ (M_r = 726.00): C 79.41, H 8.89, N 5.79; found: C 79.59, H 8.95, N 5.68.

Synthesis of 5

Compound **5** was prepared in a similar manner to **2** from **1** (0.446 g, 1.0 mmol) and ethyl 3-amino-4,5,6,7-tetrahydrobenzo[*b*]-thiophene-2-carboxylate (0.451 g, 2 mmol). The crude product was crystallized from toluene to afford colorless crystals of **5**, and the extract was stored at room temperature for 1 d to afford **5** as colorless crystals. An additional crop of **5** was obtained from the mother liquor. Total yield: 0.732 g (82%); m.p.: 205–208 °C; ^{1}H NMR (400 MHz, $CDCl_3$, 25 °C, TMS): δ = 7.32–6.99 (m, 6H, Ar-*H*), 5.29 (s, 1H, γ-*H*), 4.27 (m, 4H, OC*H*$_2$CH$_3$), 3.54 (s, 2H, N*H*), 3.14 (sept, 4H, C*H*Me$_2$), 2.66 (t, *J* = 7.2 Hz, 6H, OCH$_2$C*H*$_3$), 1.78 (s, 24H, CH*Me*$_2$), 1.67 (s, 6H, *Me*), 1.35 (m, 4H, C*H*$_2$), 1.24 (m, 4H, C*H*$_2$), 1.13 (m, 4H, C*H*$_2$), 0.88 ppm (m, 4H, C*H*$_2$); ^{13}C NMR (101 MHz, $CDCl_3$, 25 °C, TMS): δ = 169.19 (*C*=N), 161.20 (*C*OOCH$_2$CH$_3$), 161.01, 144.97, 142.29, 132.45, 125.09, 124.19, 123.02, 117.64 (*C* of Ar and thiophene), 98.05 (γ-*C*), 59.35 (OCH$_2$CH$_3$), 28.47, 28.19 (*C*HMe$_2$), 26.9, 25.36 (*C*H$_3$), 24.55, 21.22 (CH*Me*$_2$), 14.49 ppm (OCH$_2$*C*H$_3$); elemental analysis calcd (%) for $C_{51}H_{69}AlN_4O_4S_2$ (M_r = 893.20): C 68.58, H 7.79, N 6.27; found: C 68.83, H 7.89, N 6.21.

General catalytic procedure for the addition reactions of trimethylsilyl cyanide (TMSCN) to aldehydes

The catalyst (0.02 mmol), the aldehyde (1 mmol), TMSCN (1.2 mmol), and $CDCl_3$ (2 mL) were placed in a dried J. Young's Tube. The solution was stirred at ambient temperature for an appropriate time. The reaction was quenched by exposure to air. The products were identified and quantified by ^{1}H and ^{13}C NMR spectroscopy.

CCDC 1406398 (**2**), 1416414 (**3**), 1416416 (**4**), and 1416415 (**5**) contain the supplementary crystallographic data for this paper. These data are provided free of charge by The Cambridge Crystallographic Data Centre.

Acknowledgments

This work was supported by the International Science & Technology Cooperation Program of China (2014DFR61080) and the Deutsche Forschungsgemeinschaft (RO224/64-1). T.M. is thankful to the CSIR for the SRF fellowship. D.K. and S.D. acknowledge IISER-Kolkata and the CSIR project fund (01(2770/13/EMR-II) for financial support. S.D. and T.M. are grateful to Bholanath Maity for scientific discussions.

Keywords: addition reactions · aluminum complexes · DFT studies · Lewis acid catalyst

[1] H. Yamamoto, *Lewis Acids in Organic Synthesis*, Wiley-VCH, Weinheim, **2000**.

[2] a) M. Bochmann, D. M. Dawson, *Angew. Chem. Int. Ed. Engl.* **1996**, *35*, 2226 – 2228; *Angew. Chem.* **1996**, *108*, 2371 – 2373; b) D. A. Atwood, J. A. Jegier, D. Rutherford, *J. Am. Chem. Soc.* **1995**, *117*, 6779 – 6780; c) M. P. Coles, R. F. Jordan, *J. Am. Chem. Soc.* **1997**, *119*, 8125 – 8126.

[3] a) C. A. Koellner, N. A. Piro, W. S. Kassel, C. R. Goldsmith, C. R. Graves, *Inorg. Chem.* **2015**, *54*, 7139 – 7141; b) Z. Yang, M. Zhong, X. Ma, S. De, C. Anusha, P. Parameswaran, H. W. Roesky, *Angew. Chem. Int. Ed.* **2015**, *54*, 10225 – 10229; *Angew. Chem.* **2015**, *127*, 10363 – 10367.

[4] S. Saito, *Main Group Metals in Organic Synthesis* (Eds.: H. Yamamoto, K. Oshima), Wiley-VCH, Weinheim, **2004**, pp. 189 – 306.

[5] T. Ooi, K. Maruoka in *Lewis Acids in Organic Synthesis* (Ed.: H. Yamamoto), Wiley-VCH, Weinheim, **2000**, pp. 191 – 282.

[6] W. Wulff in *Lewis Acids in Organic Synthesis* (Ed.: H.Yamamoto), Wiley-VCH, Weinheim, **2000**, pp. 282 – 354.
[7] W. Li, W. Wu, Y. Wang, Y. Yao, Y. Zhang, Q. Shen, *Dalton Trans.* **2011**, *40*, 11378 – 11381.
[8] V. Jancik, Y. Peng, H. W. Roesky, J. Li, D. Neculai, A. M. Neculai, R. Herbst-Irmer, *J. Am. Chem. Soc.* **2003**, *125*, 1452 – 1453.
[9] a) V. Jancik, H. W. Roesky, D. Neculai, A. M. Neculai, R. Herbst-Irmer, *Angew. Chem. Int. Ed.* **2004**, *43*, 6192 – 6196; *Angew. Chem.* **2004**, *116*, 6318 – 6322; b) V. Jancik, H. W. Roesky, *Angew. Chem. Int. Ed.* **2005**, *44*, 6016 – 6018; *Angew. Chem.* **2005**, *117*, 6170 – 6172; c) S. P. Sarish, B. Nekoueishahraki, A. Jana, H. W. Roesky, T. Schulz, D. Stalke, *Chem. Eur. J.* **2011**, *17*, 890 – 894; d) V. Jancik, L. W. Pineda, J. Pinkas, H. W. Roesky, D. Neculai, A. M. Neculai, R. Herbst-Irmer, *Angew. Chem. Int. Ed.* **2004**, *43*, 2142 – 2145; *Angew. Chem.* **2004**, *116*, 2194 – 2197; e) P. C. Kuo, I. C. Chen, J. C. Chang, M. T. Lee, C. H. Hung, H. M. Lee, J.-H. Hung, C. H. Hu, *Eur. J. Inorg. Chem.* **2004**, *24*, 4898 – 4906; f) V. Jancik, A. P. Gómora-Figueroa, M. M. Moya-Cabrera, R. A. Toscano, R. Cea-Olivares, *Synth. React. Inorg. Met.-Org. Nano-Met. Chem.* **2007**, *37*, 741 – 744; g) V. Jancik, F. Rascón-Cruz, R. Cea-Olivares, R. A. Toscano, *Chem. Commun.* **2007**, *43*, 4528 – 4530; h) F. Rascón-Cruz, R. Huerta-Lavorie, V. Jancik, R. A. Toscano, R. Cea-Olivares, *Dalton Trans.* **2009**, *7*, 1195 – 1200; i) S. P. Sarish, H. W. Roesky, M. John, A. Ringe, J. Magull, *Chem. Commun.* **2009**, *17*, 2390 – 2392; j) V. Jancik, H. W. Roesky, *Inorg. Chem.* **2005**, *44*, 5556 – 5558; k) A. P. Gómora-Figueroa, V. Jancik, R. Cea-Olivares, R. A. Toscano, *Inorg. Chem.* **2007**, *46*, 10749 – 10753.
[10] J. A. Miller, *Chemistry of Aluminum, Gallium, Indium and Thallium* (Ed.: A. J. Downs), Chapman and Hall, London, **1993**, pp. 372 – 429.
[11] T. W. Myers, L. A. Berben, *J. Am. Chem. Soc.* **2013**, *135*, 9988 – 9990.
[12] a) M. Cheng, E. B. Lobkovsky, G. W. Coates, *J. Am. Chem. Soc.* **1998**, *120*, 11018 – 11019; b) P. L. Holland, W. B. Tolman, *J. Am. Chem. Soc.* **1999**, *121*, 7270 – 7271; c) C. Cui, H. W. Roesky, H. G. Schmidt, M. Noltemeyer, H. Hao, F. Cimpoesu, *Angew. Chem. Int. Ed.* **2000**, *39*, 4274 – 4276; *Angew. Chem.* **2000**, *112*, 4444 – 4446.
[13] a) J. C. Chang, Y. C. Chen, A. Datta, C. H. Lin, C. S. Hsiao, J. H. Huang, *J. Organomet. Chem.* **2011**, *696*, 3673 – 3680; b) M. Lamberti, I. D. Auria, M. Mazzeo, S. Milione, V. Bertolasi, D. Pappalardo, *Organometallics* **2012**, *31*, 5551 – 5560; c) L. Postigo, M. C. Maestre, M. E. G. Mosquera, T. Cuenca, G. Jiménez, *Organometallics* **2013**, *32*, 2618 – 2624; d) C. H. Huang, F. C. Wang, B. T. Ko, T. L. Yu, C. C. Lin, *Macromolecules* **2001**, *34*, 356 – 361; e) Q. Ni, L. P. Yu, *J. Am. Chem. Soc.* **1998**, *120*, 1645 – 1646; f) B. Lian, H. Ma, T. P. Spaniol, J. Okuda, *Dalton Trans.* **2009**, *41*, 9033 – 9042.
[14] a) W. Wang, Z. Yang, X. Ma, H. W. Roesky, Y. Ju, P. Hao, *Z. Anorg. Allg. Chem.* **2015**, *641*, 684 – 687; b) Z. Yang, P. Hao, X. Ma, H. W. Roesky, Y. Yang, J. Li, *Z. Anorg. Allg. Chem.* **2014**, *640*, 1081 – 1085.
[15] a) J. Casas, C. Nájera, J. M. Sansano, J. M. Saá, *Tetrahedron* **2004**, *60*, 10487 – 10496; b) J. Casas, C. Nájera, J. M. Sansano, J. M. Saá, *Org. Lett.* **2002**, *4*, 2589 – 2592; c) E. J. Campbell, H. Zhou, S. T. Nguyen, *Org. Lett.* **2001**, *3*, 2391 – 2393; d) T. Ooi, T. Miura, K. Maruoka, *Angew. Chem. Int. Ed.* **1998**, *37*, 2347 – 2349; *Angew. Chem.* **1998**, *110*, 2524 – 2526; e) I. Simpura, V. Nevalainen, *Angew. Chem. Int. Ed.* **2000**, *39*, 3422 – 3425; *Angew. Chem.* **2000**, *112*, 3564 – 3567; f) T. Yamaguchi, K. Matsumoto, B. Saito, T. Katsuki, *Angew. Chem. Int. Ed.* **2007**, *46*, 4729 – 4731; *Angew. Chem.* **2007**, *119*, 4813 – 4815.
[16] Y. Hamashima, D. Sawada, M. Kanai, M. Shibasaki, *J. Am. Chem. Soc.* **1999**, *121*, 2641 – 2642.
[17] G. Bai, Y. Peng, H. W. Roesky, J. Li, H.-G. Schmidt, M. Noltemeyer, *Angew. Chem. Int. Ed.* **2003**, *42*, 1132 – 1135; *Angew. Chem.* **2003**, *115*, 1164 – 1167.
[18] Y. Li, J. Wang, Y. Wu, H. Zhu, P. P. Samuel, H. W. Roesky, *Dalton Trans.* **2013**, *42*, 13715 – 13722.
[19] B. Qian, D. L. Ward, M. R. Smith III, *Organometallics* **1998**, *17*, 3070 – 3076.
[20] C. Cui, H. W. Roesky, H. J. Hao, H.-G. Schmidt, M. Noltemeyer, *Angew. Chem. Int. Ed.* **2000**, *39*, 4531 – 4533; *Angew. Chem.* **2000**, *112*, 4705 – 4707.

Received: December 25, 2015
Published online on April 8, 2016